

Formation mechanism of cerium oxide-doped indium oxide/Ag Ohmic contacts on *p*-type GaN

Dong-Seok Leem

School of Materials Science and Engineering, Seoul National University, Seoul 151-742, Korea

Tae-Wook Kim and Takhee Lee

Department of Materials Science and Engineering, Gwangju Institute of Science and Technology, Gwangju 500-712, Korea

Ja-Soon Jang, Young-Woo Ok, and Tae-Yeon Seong^{a)}

Division of Materials Science and Engineering, Korea University, Seoul 136-713, Korea

(Received 6 November 2006; accepted 28 November 2006; published online 28 December 2006)

The authors report on the formation of cerium oxide-doped indium oxide(2.5 nm)/Ag(250 nm) contacts to *p*-GaN. The contacts become Ohmic with a specific contact resistance of $3.42 \times 10^{-4} \Omega \text{ cm}^2$ upon annealing at 530 °C in air. X-ray photoemission spectroscopy (XPS) Ga 3*d* core levels obtained from the interface regions before and after annealing indicate a large band bending of *p*-GaN (about 1.7–1.8 eV), namely, an increase of Schottky barrier height. Based on the XPS, secondary ion mass spectroscopy, and capacitance-voltage data, possible transport mechanisms for the annealed contacts are described and discussed. © 2006 American Institute of Physics. [DOI: 10.1063/1.2424660]

Development of high-power and high-efficiency GaN light-emitting diodes (LEDs) is of technological importance for the realization of solid-state lighting.¹ For this purpose, flip-chip¹ and vertical-structure GaN-based LEDs,² *p*-side down LED structures, have been extensively investigated and shown to be effective in enhancing light extraction efficiency considerably. For such device geometries, metal reflectors with low contact resistivity are required. Among many reflectors, Ag is widely used because of its reasonable Ohmic behavior to *p*-GaN.^{3–7} However, its thermal instability upon annealing remains to be improved.³ To resolve the thermal instability, either metals or transparent conducting oxide interlayers were combined with Ag contacts. For example, Ni/Ag,^{4,5} SnO₂/Ag,⁶ and In₂O₃/Ag⁷ have been investigated. For these Ag-based contacts, Ohmic mechanisms were related to the generation of acceptorlike Ga vacancies near the *p*-type GaN surface region due to the formation of Ag–Ga solid solution.^{3,5,6} In this letter, we have investigated the addition of a CeO₂-doped In₂O₃ interlayer to Ag contacts to form low-resistance Ohmic contacts to *p*-GaN for high-performance flip-chip LEDs. Possible transport mechanisms are described in terms of combination of defect-assisted tunneling and hopping conduction via deep level defects.

1.0 μm thick *p*-type GaN layers were grown on *c*-plane sapphire substrates by metal organic chemical vapor deposition. The Hall measurement of the GaN samples showed a carrier concentration of $6.0 \times 10^{17} \text{ cm}^{-3}$ and a mobility of 10.2 cm²/V s. Prior to photolithography, the GaN samples were treated with a buffered oxide etch solution for 20 min at room temperature and rinsed in de-ionized water.⁶ Circular transmission line method patterns with an inner dot radius of 120 μm and a gap spacing of 4–24 μm were used for measuring specific contact resistance. 2.5 nm thick CeO₂-doped In₂O₃ (ICO) layers were e-beam evaporated using an In₂O₃

target containing 10 wt % CeO₂, on which Ag layers were e-beam evaporated. For reference, single Ag contacts were also prepared. Some of the samples were rapid thermal annealed at 530 °C for 1 min in air. Current-voltage-temperature (*I*-*V*-*T*) and capacitance-voltage (*C*-*V*) measurements were carried out with transfer length method patterns (100 × 50 μm² in pad size) using an HP 4155A parameter analyzer and an HP 4284A LCR meter, respectively. X-ray photoemission spectroscopy (XPS, VG Multilab ESCA 2000 model) was performed using a Mg Kα x-ray source in an UHV system. The binding energy (BE) was calibrated with respect to the Au 4*f* peak (BE=84.0 eV). Secondary ion mass spectroscopy (SIMS, Cameca IMS 6f model) was carried out using primary ion beams of cesium (C_s⁺) and oxygen (O₂⁺).

Figure 1 shows the typical *I*-*V* characteristics of ICO(2.5 nm)/Ag(250 nm) contacts before and after annealing at 530 °C. The as-deposited sample shows nonlinear *I*-*V* behavior. The electrical behavior is, however, improved significantly upon annealing. Measurements showed that the annealed sample produces specific contact resistance of $3.42 \times 10^{-4} \Omega \text{ cm}^2$. In addition, the *I*-*V*-*T* measurements were carried out and their calculated specific contact resistances are plotted as a function of the temperature, as shown in the inset of Fig. 1. Details will be discussed later.

Figure 2 shows the XPS Ga 3*d* and N 1*s* core level spectra obtained from ICO/Ag contacts on *p*-GaN before and after annealing at 530 °C. The Ga 3*d* core level obtained from the near interface region of the annealed sample shifts toward the higher binding-energy side by 1.0–1.3 eV compared to that of the as-deposited one, leading to a large band bending of *p*-GaN (about 1.7–1.8 eV),⁸ namely, an increase of Schottky barrier height. (The Ga 3*d* peak shifts indicate a change of band bending since the N 1*s* core level spectra show a shift behavior similar to that of the Ga 3*d* peaks).⁹ On the other hand, for the annealed sample, there is a shoulder at the lower binding-energy side of the Ga 3*d* peak, which is

^{a)} Author to whom correspondence should be addressed; electronic mail: tyseong@korea.ac.kr

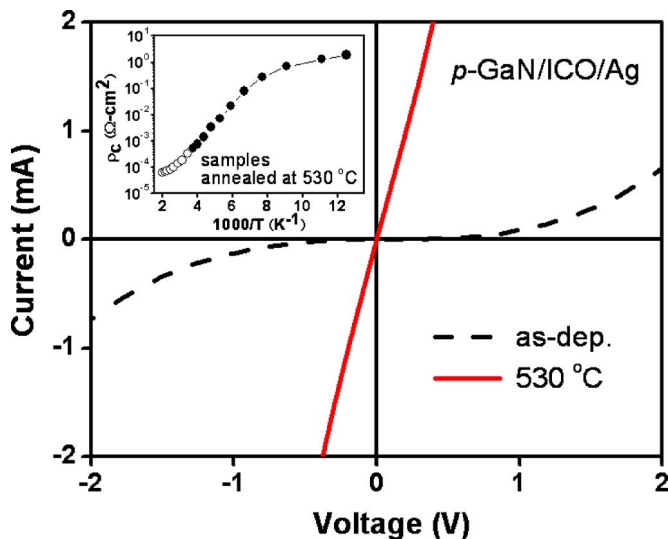


FIG. 1. (Color online) Typical I - V characteristics of ICO(2.5 nm)/Ag(250 nm) contacts to p -GaN before and after annealing at 530 °C. The specific contact resistances for the annealed sample as a function of $1/T$ are shown in the inset.

indicative of the presence of metallic Ga, which was outdiffused from GaN. This causes the generation of acceptorlike Ga vacancies at the GaN surface region.⁵ However, despite the presence of an amount of Ga vacancies below the contact, the Ga 3d peak largely shifts toward the higher binding-energy side. This implies that the surface Fermi level is affected by other defect states. This result is different from the results previously reported for Ag-based contacts.^{3,5}

SIMS depth profile results from the sample annealed at 530 °C in air (not shown) exhibited that a large amount of Ga outdiffused into the Ag layer and some amount of oxygen indiffused into GaN. This indicates that air annealing may induce active interfacial reaction and create a high density of defect states associated with Ga vacancies and oxygen-related defects.¹⁰ Thus, we believe that such defect states may cause the surface Fermi level to move to the midband gap level.⁸

Figure 3 shows the C - V characteristics of single Ag and ICO/Ag contacts after annealing at 530 °C. The capacitances of the annealed Ag contacts remain almost independent of frequency [Fig. 3(a)]. However, those of the annealed

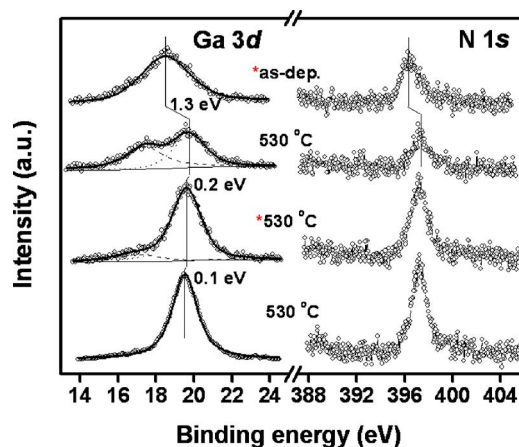


FIG. 2. (Color online) XPS spectra of Ga 3d and N 1s core levels before and after annealing at 530 °C in air as a function of the sputtering time (* denotes the midinterface region between the contact and GaN).

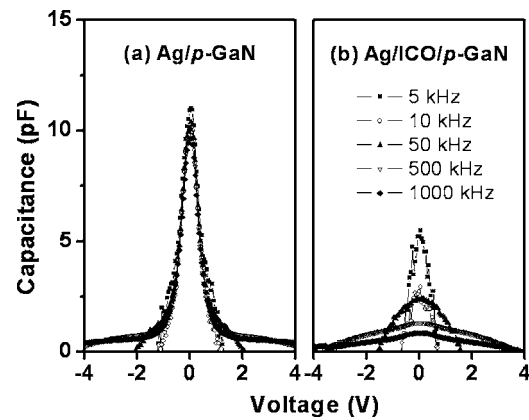


FIG. 3. Frequency dependence of the C - V characteristics of (a) the Ag and (b) ICO/Ag contacts annealed at 530 °C.

ICO/Ag contacts rapidly decrease with increasing frequency [Fig. 3(b)]. This frequency dependence shows that (deep) defect states can exist¹¹ in the annealed ICO/Ag sample, as expected from the XPS and SIMS results.

Possible transport mechanisms of the annealed ICO/Ag contacts could be described in terms of the temperature dependence of the contact resistivity as shown in the inset of Fig. 1. The contact resistivity increases with decreasing temperatures. This indicates that the carrier transport of the contacts containing a high density of defect states may be dominated by thermionic emission, defect-assisted tunneling, and hopping conduction via deep level defects.^{12,13} However, considering the large Schottky barrier height (due to a large band bending) of the annealed ICO/Ag contacts, thermionic emission could be excluded. Then, transport mechanisms may be explained by means of the defect-assisted tunneling or hopping conduction models.^{13,14}

Figure 4 shows the I - T characteristics of the annealed ICO/Ag contacts. For the defect-assisted tunneling mechanism, reverse leakage current (I) is given by¹⁴

$$I = qN_D \exp\left(-\frac{q\phi_B - \varepsilon_t}{kT}\right) \nu_{\text{ph}} W \exp(-\alpha_r W), \quad (1)$$

where N_D is the density of defect states at deep energy level (ε_t), ϕ_B the Schottky barrier height, ν_{ph} the phonon fre-

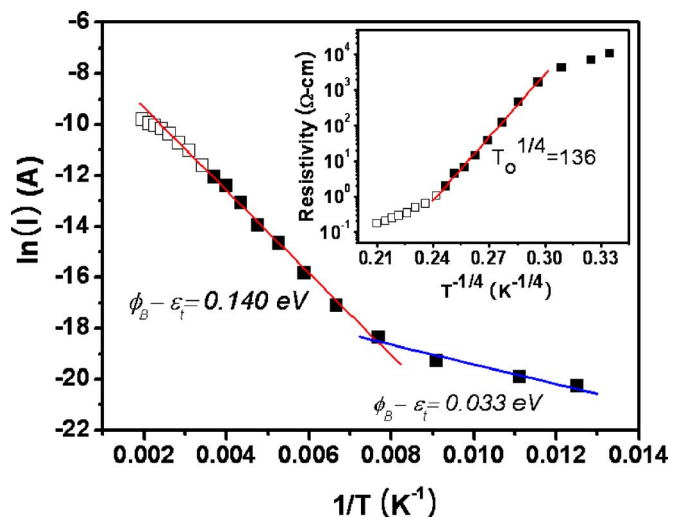


FIG. 4. (Color online) I - T characteristics of the annealed ICO/Ag contacts. The inset shows plots of the sheet resistivity of the p -GaN as a function of $1/T^{1/4}$.

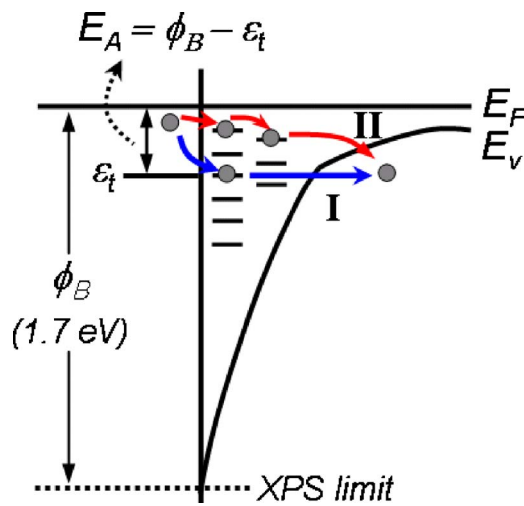


FIG. 5. (Color online) Band diagram showing possible carrier transports of ICO/Ag contacts annealed at 530 °C.

quency, W the distance between the deep defects, k the Boltzmann constant, and $\alpha_t = (2/\hbar)(2m^*\epsilon_t)^{0.5}$. The plot of $\ln I$ vs $1/T$ reveals two distinct linear fitting regions, namely, a temperature region between 413 and 130 K, and below 130 K, where their energy positions for defect-assisted tunneling ($q\phi_B - \epsilon_t$) are 0.140 and 0.033 eV, respectively. On the other hand, the temperature dependence of the sheet resistivity of p -GaN is shown in the inset of Fig. 4. In the relationship between the sheet resistivity of p -GaN and $\exp(T_0/T)^{1/4}$, where $T_0 = 16\alpha^3/kN_D$ and α^{-1} is the localization length, a linear fitting region is observed at the temperatures in the range of 293–130 K. This indicates that hopping conduction via deep level defects^{13–15} may also contribute to the carrier conduction in this temperature region.

Based on the XPS, SIMS, and electrical results, possible carrier transport mechanisms may be explained as follows. It is believed that from the I - T relation, in the temperature region 413–130 K, the carrier transport can be dominated by temperature-dependent deep defect-assisted tunneling (marked as “I” in Fig. 5) with thermal activation energy ($E_A = q\phi_B - \epsilon_t$) of 0.140 eV. For the 293–130 K region, however, hopping conduction via localized deep defect states (“II” in Fig. 5) could contribute additionally to the temperature-dependent carrier conduction. On the other hand, for the temperature region below 130 K, the relatively low tunneling energy position of 0.033 eV indicates that the

carrier transport may also be dominated by field-emission tunneling.¹³

From the XPS analysis, the large band bending of p -GaN (about 1.7–1.8 eV) attributed to the surface Fermi level pinning by a high density of defect states was observed for the sample annealed at 530 °C. This result indicated that mechanism of the oxide-combined Ag Ohmic contacts could not be explained simply by the reduction of Schottky barrier height. Instead, we proposed possible carrier conduction models via temperature-dependent defect-assisted tunneling and hopping.

In summary, we investigated the carrier transport mechanisms for the ICO(2.5 nm)/Ag(250 nm) Ohmic contacts to p -GaN by means of XPS, SIMS, and electrical measurements. It was shown that annealing caused an increase of band bending of p -GaN although the contacts became Ohmic. The C - V results indicated the presence of (deep) defect states in the annealed sample. Based on the XPS, SIMS, and electrical results, the carrier transports were described in terms of the combination of defect-assisted tunneling and hopping conduction via deep level defects.

- ¹J. J. Wierer, D. A. Steigerwald, M. R. Krames, J. J. O’Shea, M. J. Ludowise, G. Christenson, Y.-C. Shen, C. Lowery, P. S. Martin, S. Subramanya, W. Gotz, N. F. Gardner, R. S. Kern, and S. A. Stockman, *Appl. Phys. Lett.* **78**, 3379 (2001).
- ²W. Y. Lin, D. S. Wu, K. F. Pan, S. H. Huang, C. E. Lee, W. K. Wang, S. C. Hsu, Y. Y. Su, S. Y. Huang, and R. H. Horng, *IEEE Photonics Technol. Lett.* **17**, 1809 (2005).
- ³J.-O. Song, J. S. Kwak, Y. Park, and T.-Y. Seong, *Appl. Phys. Lett.* **86**, 062104 (2005).
- ⁴H. S. Venugopalan, X. Gao, T. Zhang, B. S. Shelton, A. Dicarolo, I. Eliashevich, and M. Hsing, *Proc. SPIE* **5187**, 260 (2004).
- ⁵H. W. Jang and J.-L. Lee, *Appl. Phys. Lett.* **85**, 5920 (2004).
- ⁶D.-S. Leem, J.-O. Song, H.-G. Hong, J. S. Kwak, Y. Park, and T.-Y. Seong, *Electrochem. Solid-State Lett.* **7**, G219 (2004).
- ⁷J.-O. Song, D.-S. Leem, J. S. Kwak, O. H. Nam, Y. Park, and T.-Y. Seong, *IEEE Photonics Technol. Lett.* **16**, 1450 (2004).
- ⁸T. Hashizume, *J. Appl. Phys.* **94**, 431 (2003).
- ⁹K. M. Tracy, P. J. Hartlieb, S. Einfeldt, R. F. Davis, E. H. Hurt, and R. J. Nemanich, *J. Appl. Phys.* **94**, 3939 (2003).
- ¹⁰J. Elsner, R. Jones, M. I. Heggie, P. K. Sitch, M. Haugk, Th. Frauenheim, S. Oberg, and P. R. Briddon, *Phys. Rev. B* **58**, 12571 (1998).
- ¹¹K. Liu, C. Johnston, J. H. Chu, S. Roth, B. Zhang, and M. Wan, *J. Appl. Phys.* **82**, 286 (1997).
- ¹²E. H. Rhoderick and R. H. Williams, *Metal-Semiconductor Contacts* (Clarendon, Oxford, 1988), p. 77.
- ¹³E. J. Miller, E. T. Yu, P. Waltereit, and J. S. Speck, *Appl. Phys. Lett.* **84**, 535 (2004).
- ¹⁴S. S. Simeonov and E. Kafedjijska, *Semicond. Sci. Technol.* **12**, 1016 (1997).
- ¹⁵D. C. Look, D. C. Reynolds, W. Kim, O. Aktas, A. Botchkarev, A. Salvador, and H. Morkoc, *J. Appl. Phys.* **80**, 2960 (1996).